

Hard/soft selectivity in ligand substitution reactions of β -diketonate platinum(II) complexes†

Sandra A. De Pascali,^a Paride Papadia,^a Serena Capoccia,^a Luciano Marchiò,^b Maurizio Lanfranchi,^b Antonella Ciccarese^a and Francesco P. Fanizzi^{*a,c}

Received 11th May 2009, Accepted 7th July 2009

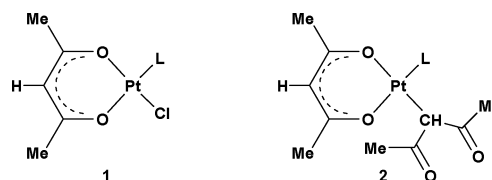
First published as an Advance Article on the web 31st July 2009

DOI: 10.1039/b909209a

The reactivity of platinum(II) complexes of the type [PtCl(*O,O'*-acac)(L)] (**1**) and [Pt(*O,O'*-acac)(γ -acac)(L)] (**2**) (L = DMSO, **a**; DMS, **b**), with a range of hard and soft nucleophiles such as dimethylsulfide (DMS, **b**), triphenylphosphine, (PPh₃, **c**), ethylene (η^2 -C₂H₄, **d**), carbon monoxide (CO, **e**), pyridine (py, **f**), and guanosine (Guo, **g**) has been investigated. Interestingly, the complexes **1a** and **1b** undergo selective substitution of the chloro or sulfur ligand depending on the hard/soft character of the incoming nucleophile. The soft incoming ligand replaces the softer one and the hard ligand replaces the harder one, giving [PtCl(*O,O'*-acac)(L)] complexes (**1b**, **1c**, **1d** and **1e** in the reaction of **1a** with L = DMS, PPh₃, η^2 -C₂H₄, CO, respectively), and [Pt(*O,O'*-acac)(DMSO)(L')] (**3f**, **3g**) and [Pt(*O,O'*-acac)(DMS)(L')] (**4f**, **4g**) species in the reaction of **1a** and **1b** with L' = py and guo, respectively. In the cases of **2a** and **2b** complexes, where the σ -bonded acac (γ -acac) replaces the chloro ligand, only in the presence of an incoming soft nucleophile substituting the soft sulfur ligand the reaction occurs. Equilibrium constants for the substitution reactions were measured by ¹H NMR spectroscopy. Variable temperature ¹H NMR spectroscopy studies, performed for the reaction of **1a** and **2a** complexes with DMS, revealed that the selective substitution of DMSO with DMS takes place in both cases, according to a second-order kinetic law. The calculated values of ΔH^\ddagger and ΔS^\ddagger are consistent with an associative mechanism. NMR spectroscopic characterization (¹H, ¹³C, ¹⁹⁵Pt, ³¹P) for the complexes and crystal structures of isolated complexes ([PtCl(*O,O'*-acac)(L)] (**1**) and [Pt(*O,O'*-acac)(γ -acac)(L)] (**2**), L = DMSO, **1a** and **2a**; L = DMS, **1b** and **2b**; L = PPh₃, **1c** and **2c**) are herein reported and discussed.

Introduction

Recently, we have reported the synthesis of a novel family of Pt(II) β -diketonate complexes, which exhibit cytotoxic activity higher than cisplatin on several cancer cell lines.¹ Interestingly, the activity appears to be related to the reaction with non-genomic biological targets.^{2–4} These complexes contain a single chelated (*O,O'*-acac) (**1**), or one chelated and one σ -bonded (γ -acac)^{5,6} (**2**) acetylacetonate. The coordination sphere is completed by one chloride (Cl[−]) and one sulfur ligand (dimethylsulfoxide, DMSO, **1a**, or dimethylsulfide, DMS, **1b**), or simply by the soft sulfur ligand (DMSO, **2a** or DMS, **2b**) in type **1** and **2** complexes, respectively (Scheme 1). The [PtCl(*O,O'*-acac)(DMS)] (**1b**) and [Pt(*O,O'*-acac)(γ -acac)(DMS)] (**2b**) complexes were easily prepared by reaction of [PtCl(*O,O'*-acac)(DMSO)] (**1a**) and [Pt(*O,O'*-acac)(γ -acac)(DMSO)] (**2a**) with excess DMS. Interestingly, in



Scheme 1 Chemical structure of *O,O'*-chelated acac complexes: **1a** and **2a**, L = DMSO; **1b** and **2b**, L = DMS.

the case of [PtCl(*O,O'*-acac)(DMSO)] (**1a**), this substitution is selective for the softer DMSO among the two possible leaving ligands (DMSO and Cl[−]).

Selectivity in ligand substitution reactions is an important topic, widely studied in coordination and organometallic chemistry. The *trans*^{7,8} and *cis*^{9,10} effects have often been used in order to explain selectivity in substitution reactions involving square-planar Pt(II) complexes.

However, in most cases the studied systems were characterized by the presence of amines as non-leaving ligands. Selective substitution reactions of Pt(II) complexes with soft ligands have been previously reported for systems having four monodentate ligands coordinated to the metal in a square planar arrangement.^{11–14} Moreover, selective substitution of the π bonded Hacac (enolic form) with soft (olefins, CO, PPh₃) and hard (py) ligands, was also observed for [PtCl(*O,O'*-acac)(η^2 -Hacac)], obtained from [PtCl(*O,O'*-acac)(γ -acac)][−] by protonation of the σ

^aDipartimento di Scienze e Tecnologie Biologiche ed Ambientali, Università del Salento, prov.le Lecce/Monteroni, I-73100, Lecce, Italy. E-mail: fp.fanizzi@unisalento.it; Fax: +39 832 298 626; Tel: +39 832 298 867

^bDipartimento di Chimica Generale ed Inorganica, Chimica Analitica, Chimica Fisica, Parco Area delle Scienze 17A, 43100, Parma, Italy

^cConsortium C.A.R.S.O., Cancer Research Center, I-70100, Valenzano-Bari, Italy

† Electronic supplementary information (ESI) available: Selected bond lengths and angles for **1a–1c**, selected bond lengths and angles for **2a–2c**, plot of pseudo-first-order rate constants as a function of [DMS] for reaction **1a**→**1b**. CCDC reference numbers 713088–713093. For ESI and crystallographic data in CIF or other electronic format see DOI: 10.1039/b909209a

bonded γ -acac.¹⁵ On the other hand the reaction of [PtCl(en)(L)]Cl (en = N,N'-chelate ethylenediamine, L = DMSO, DMS) with a range of charged and neutral, soft or hard nucleophiles,^{16,17} regularly results in the substitution of the chloro ligand. In this context, our *O,O'*-acac chelate complexes represent, to the best of our knowledge, the first Pt(II) complexes with a symmetric *O,O'*-donor carrier ligand showing selective reactivity towards hard or soft nucleophiles. In this work, the peculiar reactivity of the novel acac complexes has been studied from the kinetic and thermodynamic viewpoint and extended with a range of hard and soft nucleophiles such as dimethylsulfide (DMS), triphenylphosphine (PPh₃), ethylene (η^2 -C₂H₄), carbon monoxide (CO), pyridine (py), and guanosine (Guo). NMR characterization (¹H, ¹³C, ¹⁹⁵Pt, and ³¹P) and crystal structures are reported and discussed for all isolated complexes ([PtCl(*O,O'*-acac)(L)] (**1**) and [Pt(*O,O'*-acac)(γ -acac)(L)] (**2**), L = DMSO, **1a** and **2a**; L = DMS, **1b** and **2b**; L = PPh₃, **1c** and **2c**). Where possible, equilibrium and kinetic constants for the substitution reactions (monitored by ¹H NMR spectroscopy) have been measured. Moreover, activation parameters (ΔH^\ddagger , ΔS^\ddagger and ΔG^\ddagger) for the DMSO substitution by DMS for **1a** and **2a** complexes have been obtained by variable temperature ¹H NMR spectroscopy.

Results and discussion

Synthesis and NMR spectroscopy characterization

The synthesis and the spectroscopic characterization of **1a** and **2a** complexes were previously reported,² their crystal structures will be here discussed. The synthetic procedures of **1b-2b** and

1c-2c complexes reported in the experimental section were developed, taking advantage of the selective reactivity showed by **1a-2a** compounds towards soft nucleophiles. Indeed, [PtCl(*O,O'*-acac)(DMSO)] (**1a**) and [Pt(*O,O'*-acac)(γ -acac)(DMSO)] (**2a**) complexes give selective substitution of DMSO in the presence of incoming soft ligand such as DMS or PPh₃. For the synthesis of **1b** and **2b** complexes, an excess of DMS was added to **1a** and **2a**, in order to complete the substitution reaction. However, in the case of **1c** and **2c**, a stoichiometric amount of PPh₃ is required, in order to avoid the further chloride substitution leading to the coordination of a second phosphine ligand. Interestingly, [Pt(*O,O'*-acac)(γ -acac)(PPh₃)] (**2c**) was previously obtained only by reaction of [Pt(*O,O'*-acac)₂] with PPh₃.^{18,19} The substitution reaction of the soft sulfur ligand was also used to obtain the ethylene (**1d-2d**) and CO (**1e-2e**) species by reacting **1a-2a** or **1b-2b** in the presence of excess gaseous ligand. Complexes (**1b-2b** and **1c-2c**) were isolated and characterized by ¹H, ¹³C, ¹⁹⁵Pt, and ³¹P NMR spectroscopy and X-ray diffraction crystal structure. The ethylene (**1d-2d**) and CO (**1e-2e**) complexes were characterized in solution by ¹H NMR. Relevant NMR data for all complexes are reported in Table 1 (¹H), Table 2 (¹³C), and Table 3 (¹⁹⁵Pt). ¹H NMR spectra of **1c**, **1d**, **1e**, **2c** and ¹³C NMR spectra of **2c** were found consistent with those already reported.^{15,18,19} The ¹H NMR spectra in CDCl₃ of **1b-e** and **2b-e** complexes show the characteristic signal pattern of an asymmetric *O,O'*-acac chelate already observed for **1a-2a**. This consists of two singlets, assigned to the two methyl groups, and one more deshielded singlet for γ CH, in agreement with the aromatic character of the *O,O'*-acac chelate metalla-cycle. NOE cross-peaks with DMS or PPh₃ hydrogens in the 2D ¹H NOESY spectra of **1b-2b** and **1c-2c** allow to assign the lower frequency

Table 1 ¹H NMR chemical shifts of acac complexes with soft/hard ligand^a

	Solvent	H/C γ	Me/acac	L = DMSO, DMS, PPh ₃ , η^2 -C ₂ H ₄ , py, guo
1a	CDCl ₃	5.56 (O-bonded)	2.06; 2.02 [#] (O-bonded)	3.44 [40]* (DMSO)
	CD ₃ OD	5.56 (O-bonded)	2.05; 2.02 [#] (O-bonded)	3.45 [20] (DMSO)
2a	CDCl ₃	5.53 (O-bonded)	2.00; 1.95 [#] (O-bonded)	3.31 [19] (DMSO)
	CD ₃ OD	4.79 [120] (γ -bonded)	2.29 (γ -bonded)	
1b	CDCl ₃	5.69 (O-bonded)	2.01; 2.00 [#] (O-bonded)	3.35 [20] (DMSO)
	CD ₃ OD	4.82 [120] (γ -bonded)	2.26 (γ -bonded)	
1b	CDCl ₃	5.48 (O-bonded)	1.97; 1.88 [#] (O-bonded)	2.34 [48] (DMS)
	CD ₃ OD	5.62 (O-bonded)	1.92; 1.90 [#] (O-bonded)	2.31 [47] (DMS)
2b	CDCl ₃	5.47 (O-bonded)	1.95; 1.89 [#] (O-bonded)	2.29 [51] (DMS)
	CD ₃ OD	4.88 [124] (γ -bonded)	2.20 (γ -bonded)	
1c	CDCl ₃	5.62 (O-bonded)	1.96; 1.95 [#] (O-bonded)	2.31 [50] (DMS)
	CDCl ₃	4.90 [120] (γ -bonded)	2.19 (γ -bonded)	
1c	CDCl ₃	5.39 (O-bonded)	2.02; 1.47 [#] (O-bonded)	7.73m <i>o</i> , 7.39m <i>m</i> , 7.45m <i>p</i> , (PPh ₃) δ^{31} P = 0.40, J_{Pt-P} = 4195
	CDCl ₃	5.42 (O-bonded)	1.98; 1.52 [#] (O-bonded)	7.69m <i>o</i> , 7.40m <i>m</i> , 7.45m <i>p</i> (PPh ₃) δ^{31} P = 4.51, J_{Pt-P} = 4492
1d	CDCl ₃	3.94 dd (5.8)♦ [110] (γ -bonded)	2.13 (γ -bonded)	
	CDCl ₃	5.55 (O-bonded)	2.16; 1.95 [#] O-bonded	4.47[64] (η^2 -C ₂ H ₄)
2d	CDCl ₃	5.53 (O-bonded)	2.10; 1.96 [#] O-bonded	4.02[65] (η^2 -C ₂ H ₄)
	CDCl ₃	3.88[114] (γ -bonded)	2.22 γ -bonded	
1e	CDCl ₃	5.68 (O-bonded)	2.12; 2.10 [#] (O-bonded)	
	CDCl ₃	5.63 (O-bonded)	2.08; 2.06 [#] (O-bonded)	
2e	CDCl ₃	4.59 [132] (γ -bonded)	2.27 (γ -bonded)	
	CDCl ₃	5.48 (O-bonded)	1.94; 1.87 O-bonded	3.46 [20] (DMSO); 8.75 [40]m <i>o</i> , 7.43m <i>m</i> , 7.87m <i>p</i> (py)
3f	CD ₃ OD	5.92 (O-bonded)	2.14; 2.06 O-bonded	3.48 [20] (DMSO); 8.84 [40]m <i>o</i> , 7.62m <i>m</i> , 8.13m <i>p</i> (py)
	D ₂ O	5.99 (O-bonded)	2.12; 2.00 O-bonded	3.52–3.51; 3.40–3.39 (DMSO); 8.62 H8, 5.99 H1' (guo)
3g	CD ₃ OD	5.95 (O-bonded)	2.14; 2.05 O-bonded	3.51–3.50; 3.40–3.49 (DMSO); 8.72 H8, 5.95 H1' (guo)
	CDCl ₃	5.50 (O-bonded)	1.93; 1.86 O-bonded	2.43 [42] (DMS); 8.83 [34]m <i>o</i> , 7.36m <i>m</i> , 780m <i>p</i> (py)
4f	CDCl ₃	5.50 (O-bonded)	1.93; 1.86 O-bonded	2.43 [42] (DMS); 8.83 [34]m <i>o</i> , 7.36m <i>m</i> , 780m <i>p</i> (py)
	CD ₃ OD	5.78 (O-bonded)	2.06; 1.97 O-bonded	2.41; 2.39 (DMS); 8.61 H8, 5.93 H1' (guo)

^a # indicates the acac methyl group *cis* to the L ligand. J_{H-P} (♦) and J_{H-Pt} (*) are reported in parentheses (Hz) and in square brackets [Hz], respectively, where measurement was possible.

Table 2 ^{13}C NMR chemical shifts (δ) of isolated complexes

	C/(<i>O,O'</i> -acac)	C/(σ -acac)	C/L ligand
1a	26.3 (Me), 102.3 (γCH) 185.1 [#] , 185.9 (C=O)		44.3 (DMSO)
2a	27.50, 27.3 [#] (Me), 102.2 (γCH) 185.8 [#] , 184.9 (C=O)	30.9 (Me) 42.0 (γCH) 208.5 (C=O)	42.95 (DMSO)
1b	26.5, 26.1 [#] (Me), 101.7 (γCH) 184.9, 182.9 [#] (C=O)		22.1 (DMS)
2b	27.1, 27.5 [#] (Me), 101.6 (γCH) 183.7, 184.7 [#] (C=O)	30.9 (Me), 40.5 (γCH) 207.2 (C=O)	22.1 (DMS)
1c	27.3, 25.8 [#] (Me), 101.4 (γCH) 185.7, 183.0 [#] (C=O)		134.6 (<i>o</i>), 128.0 (<i>m</i>), 130.9 (<i>p</i>)(PPh ₃)
2c	27.8, 26.9 [#] (Me), 100.9 (γCH) 183.9, 184.1 [#] (C=O)	30.9 (Me), 41.1 (γCH) 209.1 (C=O)	134.4 (<i>o</i>), 127.9 (<i>m</i>), 130.7 (<i>p</i>)(PPh ₃)

[#] # indicates the acac methyl group *cis* to the L ligand.

Table 3 ^{195}Pt NMR chemical shifts of isolated acac complexes

	δ
1a	-2399
2a	-3198
1b	-2096
2b	-2905
1c	-2888 [4195] ^a
2c	-3532 [4492] ^a

^a $J_{\text{P-Pt}}$ are reported in square brackets [Hz].

signal of the two methyl groups to the methyl in *cis* to the soft ligand (DMS/PPh₃).

Due to the PPh₃ phenyl groups' anisotropic effect, the *O,O'*-acac chelate methyl *cis* to PPh₃ is significantly more shielded with respect to the analogous methyl in the other complexes. Therefore, the two singlets of the *O,O'*-acac methyl groups in the phosphine complexes **1c** and **2c** (2.02 and 1.47, 1.98 and 1.52 ppm for **1c** and **2c**, respectively) exhibit the greater $\Delta\delta$ (-0.5 ppm) with respect to the analogous complexes. The lower frequency resonance of *O,O'*-acac methyl group was assigned to the methyl in *cis* to the L ligand, by comparing the ^1H NMR data of **2d** and **2e** species with those already reported for other [PtCl(*O,O'*-acac)(L)] complexes (L = olefin, tertiary phosphine, carbon monoxide).^{15,20-23} The ^1H NMR spectra of **2b-e** complexes exhibit for the $\text{C}\gamma\text{-H}$ acac the characteristic deshielded signal with ^{195}Pt coupling for the methine and only one singlet relative to the methyl groups, integrating for one and six protons, respectively. Only for **2c** the methine resonance is a doublet, due to the ^{31}P coupling ($\delta = 3.94$, $^3J_{\text{H-P}} = 5.8$ Hz and a $^2J_{\text{H-Pt}} = 110$ Hz). The spectra of **1b** and **2b** show only one singlet for two methyl groups of the DMS ligand with the characteristic ^{195}Pt coupling ($\delta = 2.29$ with a $^3J_{\text{H-Pt}}$ of 51 Hz and $\delta = 2.31$ with a $^3J_{\text{H-Pt}}$ of 50 Hz for **1b** and **2b**, respectively). The **1c-2c** complexes exhibit at high frequencies the characteristic triphenylphosphine signal pattern and in the ^{31}P NMR spectra they show only one signal at 0.40 and 4.51 ppm with a $^1J_{\text{P-Pt}}$ of 4195 and 4492 Hz for **1c** and **2c**, respectively. In the ^1H NMR spectra of **1d** and **2d** complexes the singlets at 4.47 ($^2J_{\text{H-Pt}}$ of 64 Hz) and 4.02 ppm ($^2J_{\text{H-Pt}}$ of 65 Hz), respectively,

account for the ethylene group. The ^{13}C NMR spectra, acquired for isolated complexes, confirmed the structures assigned on the basis of ^1H NMR spectroscopic data. One bond and long range 2D ^1H - ^{13}C HETCOR experiments allowed correct assignments for all the ^{13}C resonances. In particular, *O,O'*-chelated and $\text{C}\gamma$ -bonded acac groups show very different chemical shifts for the $\text{C}\gamma$ atom. The pseudo-aromatic $\text{C}\gamma$ carbons of the acac chelates resonate downfield with respect to the corresponding carbon in the σ -bonded acac (see Table 2). Carbonyls of the acac chelate involved in the pseudo-aromatic metallacycle resonate at lower frequencies with respect to the σ -bonded acac ones. The long range 2D ^1H - ^{13}C HETCOR spectra, together with the above mentioned NOESY data, were used to correlate the carbonyls and the methyl groups belonging to the same half of the asymmetric chelate acac. Due to the substitution of the Cl^- with the strong σ -donor γ -acac ligand, the ^{195}Pt spectra of the isolated species **2a-c** show a more deshielded signal (*ca.* 600–800 ppm $\Delta\delta$) with respect to **1a-c** complexes (Table 3). As already observed for other Pt phosphino-complexes,²⁴ the **1c-2c** phosphino species exhibit the greater ^{195}Pt shielding with respect to the sulfur complexes **1a-2a** and **1b-2b**. Furthermore, for both type **1** and **2** complexes the shielding of ^{195}Pt chemical shift follows the series PPh₃ > DMSO > DMS according to the soft ligand substitution (DMSO in **a**, DMS in **b**, and PPh₃ in **c**).

Crystal structure

Molecular drawings and crystal packing of **1a**, **1b**, and **1c** are depicted in Fig. 1–3, whereas selected bond lengths and angles are reported in Table S1.† In all complexes the Pt atom shows a square-planar coordination achieved by means of a *O,O'*-chelate acetylacetonate ligand, a chlorine atom, and a S-coordinated DMSO (**1a**), a S-coordinated DMS (**1b**), or a PPh₃ molecule (**1c**). Two independent molecules stacked through the Pt-acac hexa-atomic ring are present in **1a**. The Pt atoms of the two complexes exchange two long contacts with the oxygen atoms *trans* to the chlorine atom of the other complex (Pt–O range 3.610(7)–3.783(7) Å). This generate 1D chains that run parallel to the *b* crystallographic axis (Fig. 1). On the contrary, in the crystal packing of **1b**, adjacent molecules are arranged perpendicularly to each other (Fig. 2). In the case of **1c**, the asymmetric unit contains two independent complexes (Fig. 3) and the main difference between them is represented by the arrangement of the phenyl residues of the PPh₃ ligand. In fact, the C(32) atom of one phenyl ring, belonging to unit-1, points towards the Cl(2) atom of the other complex, whereas the corresponding C(36) atom of unit-2 points towards the O(21) oxygen atom. In **1a**, **1b** and **1c** complexes, the Pt–O bond distance *trans* to the chlorine atom is slightly shorter than the one *trans* to the sulfur or phosphorous atom, suggesting a greater *trans* influence of the DMSO, DMS, or PPh₃ moieties with respect to Cl^- .²⁵ The bond lengths within the acetylacetonate unit are in agreement with the π delocalization of the six-membered ring. In **1a** the two independent molecules show practically the same bond distances and angles, and they are comparable with those of **1b**, apart from the Pt–S bond distance that reflects the different electronic configuration of the S atoms in DMSO and DMS (Table S1†).²⁶

The molecular drawings of **2a**, **2b** and **2c** are reported in Fig. 4–6 and selected bond lengths and angles are reported in

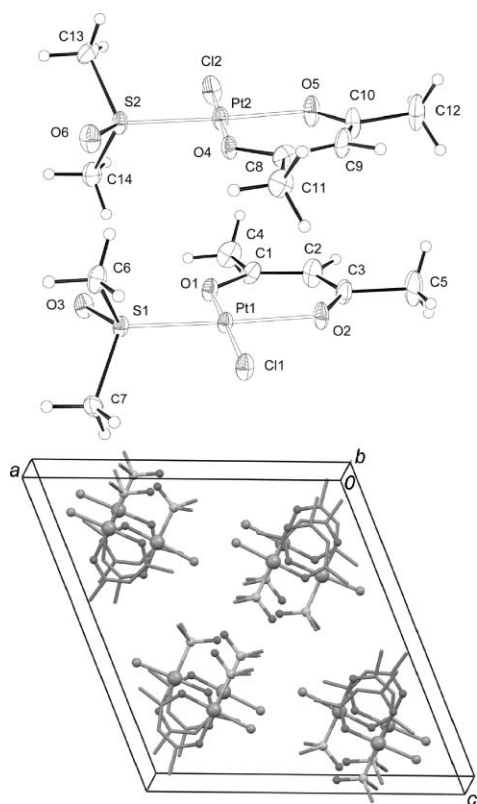


Fig. 1 Molecular structure of **1a** showing the two independent complexes. Thermal ellipsoids are drawn at the 30% probability level (above); crystal packing of **1a** projected along the *b* crystallographic axis. Hydrogen atoms were removed for clarity (below).

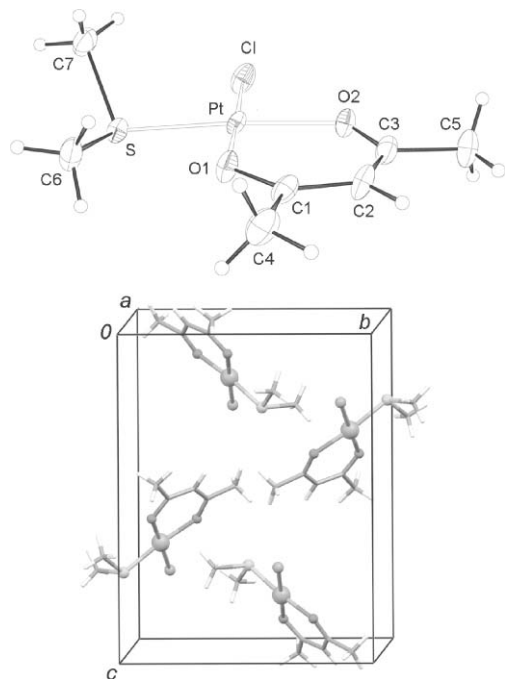


Fig. 2 Molecular structure of **1b**. Thermal ellipsoids are drawn at the 30% probability level (above); crystal packing of **1b** projected along the *a* crystallographic axis (below).

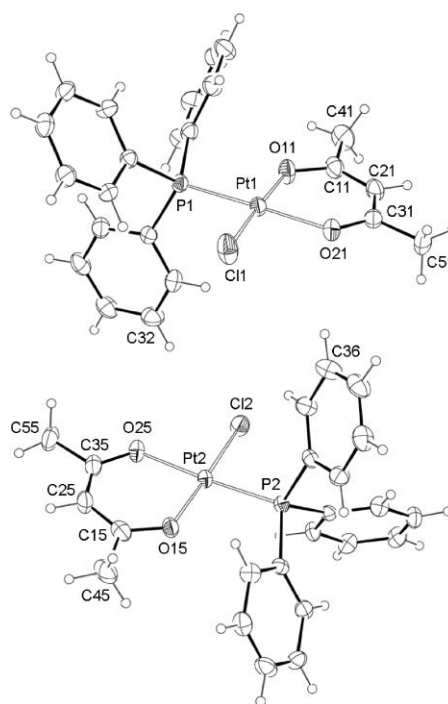


Fig. 3 Molecular structure of **1c**. Thermal ellipsoids are drawn at the 30% probability level. The two complex molecules that represent the asymmetric unit are reported.

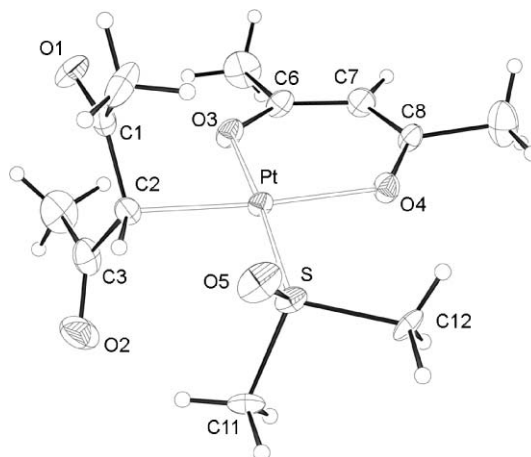


Fig. 4 Molecular structure of **2a**. Thermal ellipsoids are drawn at the 30% probability level.

Table S2.† The molecular structure of **2a** was recently reported showing an asymmetric unit comprised of three molecular units (space group $P-1$).² In the present case, the asymmetric unit is represented by one complex molecule (space group $P2_1/n$) and the geometric parameters are essentially equivalent with those previously reported (Fig. 4). In these complexes the square planar coordination of the metal is defined by one O,O' chelate acetylacetonate ligand, a $C\gamma$ -bonded acetylacetonate, and a S-coordinated DMSO (**2a**), a DMS (**2b**), or a PPh_3 molecule (**2c**). The bidentate acetylacetonate moiety presents bond lengths that are in agreement with the π delocalization as found for **1a-c**, whereas the $C\gamma$ bonded one exhibits a tetrahedral geometry at the $C\gamma$ carbon atom, and C-O distances consistent with a

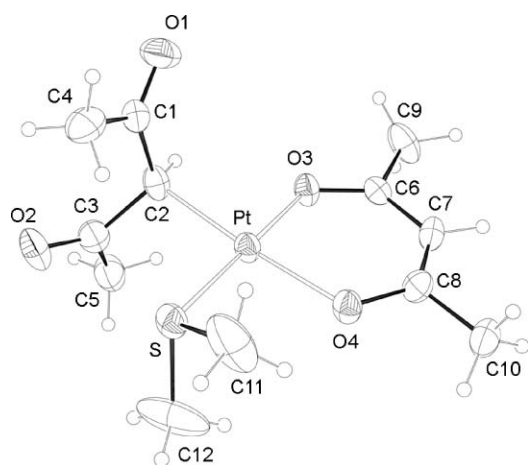


Fig. 5 Molecular structure of **2b**. Thermal ellipsoids are drawn at the 30% probability level.

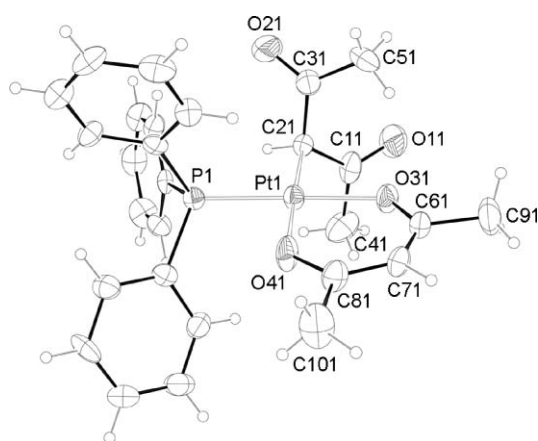


Fig. 6 Molecular structure of **2c**. Thermal ellipsoids are drawn at the 30% probability level. One of the two independent molecules is reported.

double bond character (Table S2[†]). The main difference between **2a** and **2b** is represented by the orientation of the C γ bonded acetylacetonate ligand with respect to the S-donor one. In fact, in **2a**, the C γ -H is directed towards the DMSO molecule and is bisecting the O(5)-S-C(11) angle, whereas in **2b** it is oriented towards the O(3) atom of the chelate acetylacetonate ligand. As far as the Pt-O distances are concerned, **2a** exhibits the longer distance for the bond in *trans* to the DMSO molecule, whereas in **2b** and **2c**, the longer Pt-O distances are those in *trans* to the C γ carbon. This is a consequence of the greater *trans* influence of the C γ -bonded acetylacetonate group with respect to the chloride ion that is present in **1a-c**. Interestingly, the asymmetric unit of **2c** is comprised of two complex molecules that are strictly related by a pseudo-center of symmetry, and on a first stage, this cast some doubts on the space group assignment (Fig. 7). Nevertheless, by inspecting the crystal packing it became evident that this symmetry is only local, since it does not apply to the rest of the lattice but only to the two molecular units. As an example, the C(251) atom of unit-1 points towards the center of the penta-atomic ring containing Pt(2)'', whilst the pseudo-centrosymmetric C(212) atom points towards O(11)'. Interestingly, the Pt-O distances *trans* to the phosphorus or sulfur in type **1** ($\text{PPh}_3 > \text{DMSO} \geq \text{DMS}$) and **2** ($\text{PPh}_3 > \text{DMSO} >$

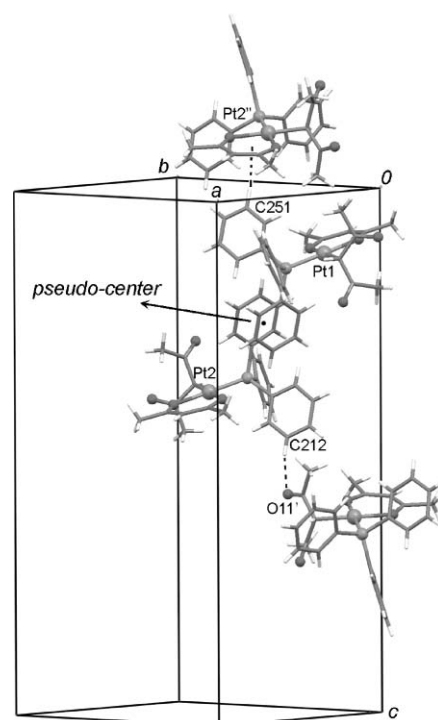


Fig. 7 Portion of the crystal packing of **2c**, with indicated the pseudo-center of symmetry. Symmetry codes: ' = x ; $-y$; $1/2 + z$, '' = x ; $1 - y$; $z - 1/2$.

DMS) account for the different *trans* influence of the soft ligands measured by crystallographic data in other model systems.²⁷

Thermodynamic and kinetic studies of the substitution reactions

Thermodynamic and kinetic studies of ligand substitution reactions with hard/soft nucleophiles for **1a-2a** and **1b-2b** were performed by ¹H NMR spectroscopy, as described in the experimental section. Reaction of [PtCl(*O, O'*-acac)(DMSO)] (**1a**) complex with DMS to give [PtCl(*O, O'*-acac)(DMS)] (**1b**) is fast in CDCl₃, reaching almost immediately the equilibrium, while reaction of [Pt(*O, O'*-acac)(γ -acac)(DMSO)] (**2a**) to give [Pt(*O, O'*-acac)(γ -acac)(DMS)] (**2b**) in the same solvent needs approximately 3 days to reach the steady-state (Fig. 8). On the other hand, comparison of the equilibrium constants evaluated by ¹H NMR spectroscopy at 25°C, for the two reactions **1a**→**1b** ($K_{1a \rightarrow 1b} = 6.5 \times 10^1 \pm 1.3 \times 10^1$) and **2a**→**2b** ($K_{2a \rightarrow 2b} = 17.0 \times 10^1 \pm 3.4 \times 10^1$) indicates that the substitution of the sulfur ligand is thermodynamically favoured in the case of **2a** with respect to **1a**.

Therefore, although the two ligands *cis* to DMSO (Cl⁻ and γ -acac in the case of **1a** and **2a**, respectively) formally share the same charge, the strongly σ -donating ligand γ -acac favours the DMSO substitution reaction in the presence of the incoming DMSO ligand ($K_{2a \rightarrow 2b}$ greater than $K_{1a \rightarrow 1b}$). In order to rule out a solvent effect (aprotic vs. protic)²⁸ on the selectivity of the substitution, we followed the reactions of **1a** and **2a** with DMS in CD₃OD by ¹H NMR spectroscopy. The same substitution reactions (**1a**→**1b** and **2a**→**2b**) and hard/soft selectivity (leading to the exclusive DMSO over Cl⁻ substitution for **1a**→**1b**) were observed also in this case. Moreover, the reactions **1a**→**1b** and **2a**→**2b** were performed on a preparative scale to give, in the presence of excess DMS, the final

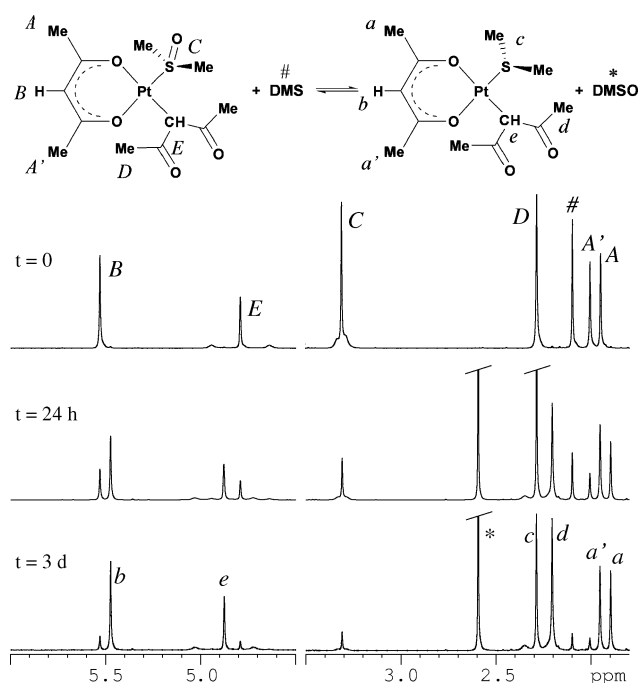


Fig. 8 ^1H NMR spectra in CDCl_3 (400 MHz) for the reaction of **2a** with DMS. $t = 0$, **2a** and free DMS; $t = 24$ h, **2a** reacts with DMS (#) giving **2b** and free DMS (*); $t = 3$ d, steady-state of the reaction.

products (**1b** and **2b**). Interestingly, these specific reactivity and selectivity have never been observed for the cationic platinum complexes $[\text{PtCl}(\text{en})(\text{DMSO})]\text{Cl}$. Indeed, when $[\text{PtCl}(\text{DMSO})(\text{en})]\text{Cl}$ (the simplest analogue of **1a**, having a chelating diamine ligand in place of a O,O' -chelated acetylacetonate) was reacted with DMS in CD_3OD , no DMSO substitution by DMS was detected. Even in the presence of excess DMS, the DMSO in $[\text{PtCl}(\text{DMSO})(\text{en})]\text{Cl}$

is slowly replaced by the counterion, affording $[\text{PtCl}_2(\text{en})]$, as normally occurs in the absence of the excess sulfur ligand.^{29,30} The kinetic constants and the activation parameters for the reactions **1a** \rightarrow **1b** and **2a** \rightarrow **2b** were also calculated by variable temperature ^1H NMR spectroscopy (in the range 288.15–308.15 K). Under the conditions reported in the experimental section, the reactions were completed in 20–60 min, and a satisfactory pseudo-first-order behaviour was observed for both reactions. The plot of pseudo-first-order rate constants, k_{obs} , against the concentration of DMS indicates a first order in the incoming ligand for both **1a** \rightarrow **1b** and **2a** \rightarrow **2b** reactions without any significant intercept. Thus, both the reactions follow the same rate law

$$k_{\text{obs}} = k_2 [\text{DMS}]$$

The second-order rate constants k_2 were obtained at different temperatures (Table 6) and were used for calculating the corresponding activation parameters, ΔG^\ddagger , ΔH^\ddagger and ΔS^\ddagger , reported in Table 7. Interestingly, the obtained data show for both reactions, within the experimental error, the same value of ΔS^\ddagger (-124 ± 6 and -124 ± 12 for **1a** \rightarrow **1b** and **2a** \rightarrow **2b**, respectively) and only a slight difference in the enthalpy contents (47 ± 2 and 50 ± 3 for **1a** \rightarrow **1b** and **2a** \rightarrow **2b**, respectively). These data imply an analogous associative mechanism for DMS promoted DMSO substitution reaction in **1a** and **2a** complexes, with a similar geometrical arrangement in the transition state.

In order to confirm the reactivity and hard/soft selectivity in the ligand substitutions for these O,O' -chelated-acac platinum systems, both the DMSO (**1a** and **2a**) and DMS (**1b** and **2b**) complexes were checked by NMR in the reactions with other soft nucleophiles such as triphenylphosphine (PPh_3), ethylene ($\eta^2\text{-C}_2\text{H}_4$) and carbon monoxide (CO) in CDCl_3 . In the presence of stoichiometric amounts of PPh_3 , both **1a** and **2a**, as well as **1b** and **2b**, gave in all cases almost immediately the substitution of the sulfur ligand and the quantitative formation of $[\text{PtCl}(O,O'\text{-acac})(\text{PPh}_3)]$

Table 4 Crystal data and structure refinement for **1a-1c**^a

	1a	1b	1c
Empirical formula	$\text{C}_7\text{H}_{13}\text{ClO}_3\text{PtS}$	$\text{C}_7\text{H}_{13}\text{ClO}_2\text{PtS}$	$\text{C}_{23}\text{H}_{22}\text{ClO}_2\text{PPt}$
Formula weight	407.77	391.77	591.92
T (K)	293(2)	293(2)	293(2)
λ (Å)	0.71073	0.71073	0.71073
Crystal system	Monoclinic	Monoclinic	Triclinic
Space group	$P2_1/c$	$P2_1/c$	$P-1$
a (Å)	17.718(11)	6.268(2)	9.948(1)
b (Å)	7.245(8)	11.781(6)	12.738(2)
c (Å)	18.793(13)	15.140(16)	18.411(2)
α (deg)	90	90	101.68(1)
β (deg)	111.57(2)	99.41(2)	100.25(1)
γ (deg)	90	90	106.83(2)
V (Å ³)	2243(3)	1103(1)	2116.0(5)
Z , ρ (calc) (Mg m^{-3})	8, 2.415	4, 2.359	4, 1.858
μ , mm^{-1}	12.907	13.115	6.849
θ range (deg)	3.01 to 27.01	3.23 to 30.00	1.17 to 26.00
Refl. Coll./uniq.	5007/4877 [$R_{\text{int}} = 0.0711$]	3314/3213 [$R_{\text{int}} = 0.0438$]	23015/8301 [$R_{\text{int}} = 0.0566$]
data/restraints/param.	4877/0/235	3213/0/113	8301/0/508
GOF on F^2	1.018	0.982	0.937
$R1$	0.0476	0.0321	0.0281
$wR2$	0.1284	0.0707	0.0449
largest diff. peak/hole ($\text{e} \text{ \AA}^{-3}$)	2.653 and -2.886	0.973 and -1.308	1.109 and -0.951

^a $R1 = \sum \|F_o\| - |F_c| / \sum |F_o|$, $wR2 = [\sum [w(F_o^2 - F_c^2)^2] / \sum [w(F_o^2)^2]]^{1/2}$, $w = 1 / [\sigma^2(F_o^2) + (aP)^2 + bP]$, where $P = [\max(F_o^2, 0) + 2F_c^2] / 3$.

Table 5 Crystal data and structure refinement for **2a-2c**^a

	2a	2b	2c
Empirical formula	C ₁₂ H ₂₀ O ₅ PtS	C ₁₂ H ₂₀ O ₄ PtS	C ₂₉ H ₃₀ Cl ₃ O ₄ PPt
Formula weight	471.43	455.43	774.94
<i>T</i> (K)	293(2)	293(2)	293(2)
λ (Å)	0.71073	0.71073	0.71073
Crystal system	Monoclinic	Monoclinic	Monoclinic
Space group	<i>P</i> 2 ₁ / <i>n</i>	<i>C</i> 2/ <i>c</i>	<i>P</i> 2/ <i>c</i>
<i>a</i> (Å)	7.910(4)	8.766(1)	17.067(6)
<i>b</i> (Å)	13.000(5)	14.185(2)	12.310(4)
<i>c</i> (Å)	15.711(8)	25.006(3)	27.577(9)
α (deg)	90	90	90
β (deg)	101.63(2)	93.561(2)	92.55(1)
γ (deg)	90	90	90
<i>V</i> (Å ³)	1582(1)	3103.4(7)	5788(3)
<i>Z</i> , ρ (calc) (Mg m ⁻³)	4, 1.979	8, 1.950	8, 1.779
μ , mm ⁻¹	9.010	9.180	5.214
θ range (deg)	3.06 to 24.99	1.63 to 26.39	1.19 to 27.00
Refl. Coll./uniq. data/restraints/param.	2878/2779 [<i>R</i> _{int} = 0.0765]	4838/3256 [<i>R</i> _{int} = 0.0000]	64056/12637 [<i>R</i> _{int} = 0.0859]
GOF on <i>F</i> ²	1.004	1.008	1.002
<i>R</i> 1	0.0409	0.0493	0.0384
<i>wR</i> 2	0.0615	0.1398	0.0526
largest diff. peak/hole (e Å ⁻³)	1.733 and -1.463	1.331 and -1.407	1.255 and -1.259

$$^a R1 = \sum \|F_o\| - |F_c| / \sum \|F_o\|, wR2 = [\sum [w(F_o^2 - F_c^2)^2] / \sum [w(F_o^2)^2]]^{1/2}, w = 1 / [\sigma^2(F_o^2) + (aP)^2 + bP], \text{ where } P = [\max(F_o^2, 0) + 2F_c^2] / 3.$$

Table 6 Kinetic constants vs. *T* for the substitution reaction of **1a** and **2a** with DMS

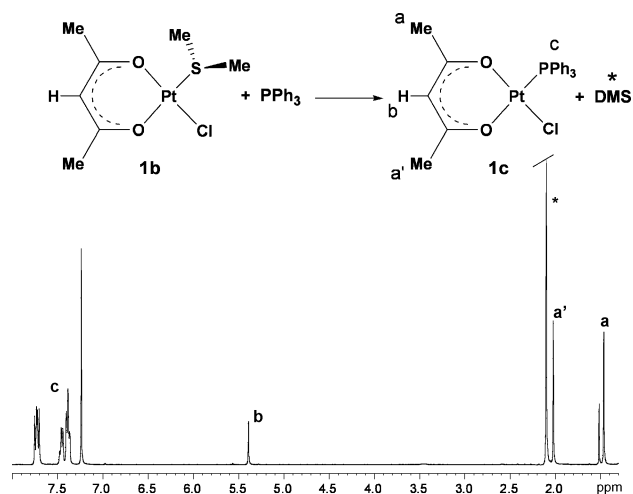
<i>T</i> (K)	<i>k</i> (1a)	Adj <i>R</i> ²	<i>k</i> (2a)	Adj <i>R</i> ²
308.15	$2.7 \times 10^{-2} \pm 1.4 \times 10^{-2}$	0.9918	$6.5 \times 10^{-3} \pm 2.9 \times 10^{-3}$	0.9771
303.15	$2.0 \times 10^{-2} \pm 1.1 \times 10^{-2}$	0.9920	$4.4 \times 10^{-3} \pm 1.7 \times 10^{-3}$	0.9833
298.15	$1.4 \times 10^{-2} \pm 0.8 \times 10^{-2}$	0.9907	$3.6 \times 10^{-3} \pm 1.3 \times 10^{-3}$	0.9951
293.15	$1.0 \times 10^{-2} \pm 0.5 \times 10^{-2}$	0.9973	$2.4 \times 10^{-3} \pm 0.8 \times 10^{-3}$	0.9992
288.15	$0.7 \times 10^{-2} \pm 0.3 \times 10^{-2}$	0.9997	$1.5 \times 10^{-3} \pm 0.5 \times 10^{-3}$	0.9989

Table 7 Activation parameters for the substitution reactions **1a**→**1b** and **2a**→**2b**

	<i>k</i> (measured at 298.15 K)	ΔH^\ddagger (kJ mol ⁻¹)	ΔS^\ddagger (J K ⁻¹ mol ⁻¹)	ΔG^\ddagger (298 K)
1a → 1b	$1.4 \times 10^{-2} \pm 0.8 \times 10^{-2}$	47 ± 2	-124 ± 6	84 ± 3
2a → 2b	$3.6 \times 10^{-3} \pm 1.3 \times 10^{-3}$	50 ± 3	-124 ± 12	87 ± 7

(**1c**) and [Pt(*O,O'*-acac)(γ -acac)(PPh₃)] (**2c**), respectively. It should be noted that also in the case of **1a** and **1b**, the PPh₃ substitution is selective for the softer ligand (DMSO/DMS) among the two possible leaving ligands (DMSO/DMS and Cl⁻) (Fig. 9). The thermodynamic of the substitution reactions (**1a/1b**→**1c** and **2a/2b**→**2c**) strongly favours the phosphino complexes **1c** and **2c**, being the equilibrium constants $K_{1a/1b \rightarrow 1c}$ and $K_{2a/2b \rightarrow 2c} \gg 10^3$, estimated from NMR data. The strongly favoured, both kinetically and thermodynamically, substitution of the sulfur ligand (DMSO or DMS) with PPh₃ allowed us to set up an easy synthetic procedure, in order to isolate in good yield **1c** and **2c** complexes.

The same reactivity and selectivity were observed also when **1a-2a** and **1b-2b** were reacted with a π -electron system nucleophile, such as ethylene (η^2 -C₂H₄) in CDCl₃. Again, the sulfur ligand displacement (DMSO or DMS) is selectively preferred over the chloride substitution in the case of **1a** and **1b**, to afford [PtCl(*O,O'*-acac)(η^2 -C₂H₄)] (**1d**) (Fig. 10), and takes place also in the case

**Fig. 9** ¹H NMR spectra in CDCl₃ for the reaction of **1b** with triphenylphosphine giving **1c**.

of **2a** and **2b** to give [Pt(*O,O'*-acac)(γ -acac)(η^2 -C₂H₄)] (**2d**). This behaviour suggests the idea that, in these systems, the driving force ruling the reactivity is the hard/soft nature of the incoming ligand.

In all the cases of sulfur ligand displacement by ethylene, the reactions are less favoured both kinetically (*ca.* two weeks are required to reach the equilibrium) and thermodynamically

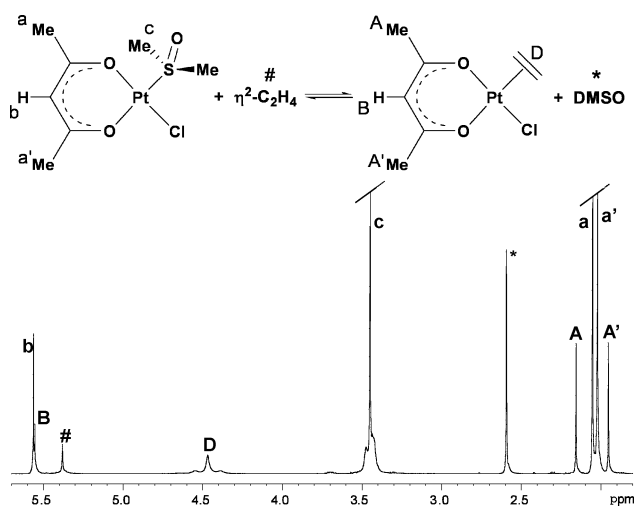


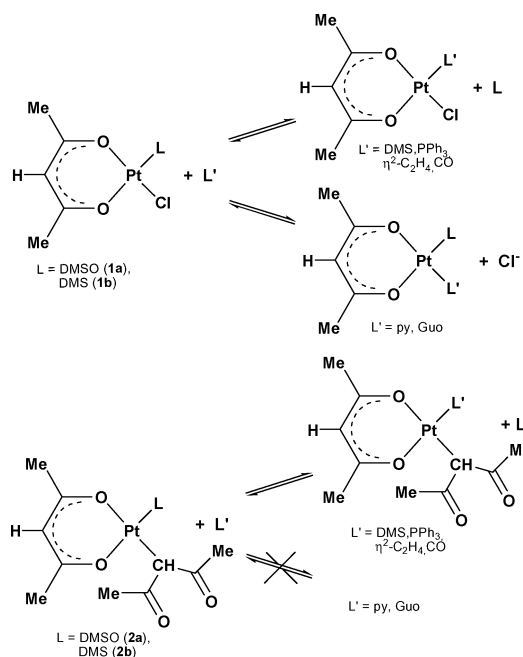
Fig. 10 ^1H NMR spectra in CDCl_3 for the reaction of **1a** with ethylene giving **1d**.

with respect to the analogous reactions, where the displacing nucleophile is another sulfur ligand or a phosphine ($K_{1a \rightarrow 1d} = 9.0 \times 10^{-1} \pm 1.8 \times 10^{-1}$, $K_{2a \rightarrow 2d} = 4.9 \times 10^{-1} \pm 9.8 \times 10^{-2}$, $K_{1b \rightarrow 1d} = 4.5 \times 10^{-2} \pm 9.0 \times 10^{-3}$ and $K_{2b \rightarrow 2d} = 3.0 \times 10^{-3} \pm 5.4 \times 10^{-4}$). The reaction of **1a-2a** and **1b-2b** with CO gave again, in all cases, substitution on the sulfur ligand. Selective displacement of DMSO or DMS over the chloro ligand from **1a** and **1b**, respectively, gave $[\text{PtCl}(\text{O},\text{O}'\text{-acac})(\text{CO})]$ (**1e**), while $[\text{Pt}(\text{O},\text{O}'\text{-acac})(\gamma\text{-acac})(\text{CO})]$ (**2e**) was obtained from **2a** and **2b**. However, in these cases, due to both the presence of CO excess and the slowness in reaching the steady-state for all four reactions, the carbonyl complexes (**1e**, **2e**) could be only spectroscopically characterized, since a further reaction takes place. Therefore, the equilibrium constants for **1a/1b** \rightarrow **1e** **2a/2b** \rightarrow **2e** reactions could not be measured, nor the pure complexes **1e** and **2e** could be isolated. In order to confirm this unforeseen reactivity and substitution selectivity for this class of compounds, we also studied by ^1H NMR spectroscopy the reaction of **1a-1b** and **2a-2b**, with hard nitrogen donor ligands such as pyridine (py) and guanosine (Guo, able to undergo easily N7 coordination). Interestingly, while **2a** and **2b** show negligible reactivity with both py and Guo, **1a** and **1b** slowly undergo chloride substitution as the first reaction step giving $[\text{Pt}(\text{O},\text{O}'\text{-acac})(\text{DMSO})(\text{py})]^+$ (**3f**), $[\text{Pt}(\text{O},\text{O}'\text{-acac})(\text{DMSO})(\text{Guo})]^+$ (**3g**) and $[\text{Pt}(\text{O},\text{O}'\text{-acac})(\text{DMS})(\text{py})]^+$ (**4f**) $[\text{Pt}(\text{O},\text{O}'\text{-acac})(\text{DMS})(\text{Guo})]^+$ (**4g**), respectively. The Cl^- substitution reactions by py or Guo appear both kinetically and thermodynamically less favoured with respect to the analogous substitutions involving the soft ligands. Moreover, at least in the case of py, even when used stoichiometrically as incoming nucleophile, NMR spectra in CDCl_3 account for further reactions involving **3f** and **4f**. These include substitution of the sulfur ligand by coordination of a second py molecule or reentering of the chloride in the Pt coordination sphere.

Conclusions

All data herein presented confirm the hypothesis that, in the 6-membered O,O' -chelate ring systems, $[\text{PtCl}(\text{O},\text{O}'\text{-acac})(\text{L})]$ (**1**) ($\text{L} = \text{DMSO}$, **a**; DMS , **b**), where, together with the O,O' -acac

carrier ligand, two leaving ligands with different hard/soft character (Cl^- and DMSO or DMS) are present, hard/soft selectivity is observed for the first substitutions. Indeed, in type **1** complexes, in the first instance, substitution of the harder leaving group by an incoming hard ligand and of the softer group by an incoming soft ligand takes place. This seems to be the case of complexes **1a** and **1b** in the reactions with another sulfur ligand, phosphine, ethylene, CO, py and Guo. On the other hand, when only a soft ligand is available for substitution (being the σ bonded γ -acac essentially unavailable for substitution in the reaction conditions) as in the cases of $[\text{Pt}(\text{O},\text{O}'\text{-acac})(\gamma\text{-acac})(\text{L})]$ (**2**) ($\text{L} = \text{DMSO}$, **a**; DMS , **b**), the substitution reaction takes place only in the presence of an incoming soft ligand, otherwise no reaction occurs at all (Scheme 2).



Scheme 2 Selective reaction of O,O' -acac complexes with soft nucleophiles and nitrogen ligands.

Kinetic and thermodynamic analyses for selective DMSO substitution by DMS indicate that both **1a** \rightarrow **1b** and **2a** \rightarrow **2b** reactions take place with a second order kinetic law and an associative mechanism with a similar geometrical configuration in the transition state. In principle, the strongly favoured substitution reactions with soft ligands, in both **1** and **2** systems can be used to set up straightforward synthetic procedures giving new O,O' -acac chelate Pt(II) complexes.

Experimental

Physical measurements

Elemental analyses were performed using a Carlo-Erba elemental analyser, model 1106. ^1H NMR, ^{195}Pt NMR, ^{31}P NMR, $^1\text{H}-^1\text{H}$ COSY, $^1\text{H}-^1\text{H}$ NOESY, $^1\text{H}-^{195}\text{Pt}$ HETCOR, $^1\text{H}-^{13}\text{C}$ HETCOR, and $^1\text{H}-^{13}\text{C}$ HETCOR long range two-dimensional experiments were recorded on a Bruker Avance DPX 400 MHz and on a Bruker Avance DRX 500 MHz (CARSO). CDCl_3 , CD_3OD , and D_2O were used as solvents, and chemical shift were referenced to TMS

for CDCl_3 and CD_3OD by the residual protic solvent peaks as internal references ($\delta = 7.24$ ppm for CDCl_3 and $\delta = 3.30$ ppm for CD_3OD) and to TSP (2,2',3,3'-d(4)-3-(trimethyl-silyl)-propionic acid sodium salt) for D_2O ($\delta = 0$ ppm) as internal reference. ^{195}Pt chemical shifts were referenced to $\text{Na}_2[\text{PtCl}_6]$ ($\delta(\text{Pt}) = 0$ ppm) in D_2O as an external reference.³¹

Starting materials

Acetylacetone (2,4-pentanedione), pyridine, guanosine, DMSO, DMS, PPh_3 , carbon monoxide, ethylene and deuterated solvents (CDCl_3 , CD_3OD , and D_2O) were used without further purification. $[\text{PtCl}(\text{en})(\text{DMSO})]\text{Cl}$,³² $[\text{PtCl}(\text{O},\text{O}'\text{-acac})(\text{DMSO})]_2$ (**1a**) and $[\text{Pt}(\text{O},\text{O}'\text{-acac})(\gamma\text{-acac})(\text{DMSO})]_2$ (**2a**) were prepared according to previously reported procedures.

Syntheses of $[\text{PtCl}(\text{O},\text{O}'\text{-acac})(\text{DMS})]$ (1b**) and $[\text{Pt}(\text{O},\text{O}'\text{-acac})(\gamma\text{-acac})(\text{DMS})]$ (**2b**).** To a chloroform (3 mL) solution of **1a** or **2a** (0.1 g, 0.24 mmol for **1a** and 0.1 g, 0.21 mmol for **2a**) a large DMS excess (0.224 g, 3.6 mmol for **1a** and 0.263 g, 4.24 mmol for **2a**) was added. The reaction mixture was left under stirring at room temperature, overnight. The resulting yellow solution was added of pentane (10 mL) and kept at 5 °C for one day up to the formation of a yellow needles crystals for **1b** and pale yellow crystals for **2b**. Finally, the crystals were isolated, washed with pentane, and dried under vacuum. (Yield 0.075 g, 0.191 mmol, 80% for **1b**. Anal. Calcd for $\text{C}_7\text{H}_{13}\text{ClO}_2\text{PtS}$ (391.773): C 21.46; H 3.34. Found: C 21.27; H 3.20; yield 0.078 g, 0.171 mmol, 82% for **2b**. Anal. Calcd for $\text{C}_7\text{H}_{13}\text{ClO}_2\text{PtS}$ (455.428): C 31.65; H 4.43. Found: C 31.72; H 4.56).

Syntheses of $[\text{PtCl}(\text{O},\text{O}'\text{-acac})(\text{PPh}_3)]$ (1c**) and $[\text{Pt}(\text{O},\text{O}'\text{-acac})(\gamma\text{-acac})(\text{PPh}_3)]$ (**2c**).** To a chloroform (30 mL) solution of **1a** or **2a** (0.1 g, 0.246 mmol for **1a** and 0.1 g, 0.212 mmol for **2a**) a stoichiometric amount of PPh_3 previously dissolved in 20 mL of CHCl_3 was added. The mixture was left under stirring at room temperature for *ca.* 6 h. The resulting solution was concentrated (5 mL) and added of pentane (20 mL) to allow the precipitation of a yellow powder for **1c** and a pale-yellow solid for **2c**. The products (**1c** and **2c**) were then collected, washed and dried under vacuum. By slow evaporation from CHCl_3 solution, yellow crystals of **1c** were obtained. Yellow crystals of **2c** were formed by addition of pentane to a CHCl_3 solution. (Yield 0.120 g, 0.202 mmol, 82% for **1c**. Anal. Calcd for $\text{C}_{23}\text{H}_{22}\text{ClO}_2\text{Ppt}$ (591.924): C 46.67 H 3.75, found C 46.10 H 3.77; yield 0.106 g, 0.162 mmol, 76% for **2c**. Anal. Calcd for $\text{C}_{28}\text{H}_{29}\text{O}_4\text{Ppt}$ (655.579): C 51.30; H 4.46, found C 50.93; H 4.45).

Reactions in NMR tube. 0.010 g of complex (**1a**, **2a**, **1b**, and **2b**) were dissolved in deuterated solvent (1 mL) and the resulting solution placed in a NMR tube. The reaction with added soft (DMS, DMSO, PPh_3 , ethylene, carbon monoxide) and hard (pyridine, guanosine) ligands in a stoichiometric amount was time-monitored recording ^1H NMR spectra. The thermodynamic measurements were performed using a Bruker Avance DPX 400 MHz at 298.15 K. The ^1H NMR spectra were conducted using a 60° pulse of 4.8 μs and a D1 delay of 5 s and 16 scans. The progress of reactions was monitored by integrating the ^1H NMR signals from the *O,O'*-acac methine of the Pt complexes.

Kinetics curve fitting and activation parameters calculation

The kinetics of reactions **1a**→**1b** and **2a**→**2b** were studied in CDCl_3 using a Bruker Avance DRX 500 MHz spectrometer equipped with an indirect broad band triple resonance probe and a variable temperature unit BVT300 module on the temperature range from 288.15 to 308.15 K. The ^1H NMR spectra were acquired using a 60° pulse of 6 μs and a D1 delay of 5 s and 8 scans. The progress of reactions was monitored by integrating the ^1H NMR signals from the *O,O'*-acac methine of the Pt complexes. The pseudo-first-order conditions were ensured by using at least 10-folds excess of DMS with respect to the Pt starting complex. The reactions were started by mixing solutions of Pt complex (0.0085 g; ~0.02 M) and DMS in CDCl_3 to give the total solution a volume of 1 mL. The pseudo-first-order constants k_{obs} were calculated from the slope of linear plots $\ln[M]$ (where $[M]$ is the concentration of starting complex) versus time (s). After preliminary fittings of the data with both the exact rate law integrated formula and the first order approximation for the studied reaction, we determined that, within the range of concentrations explored, no significant error occurred within the pseudo-first-order approximation. Therefore, for each temperature, concentration were fitted to a simple single exponential decay function, of the type $[C] = C_0 \exp(-k_{\text{obs}}t)$, where $k_{\text{obs}} = k_2[\text{DMS}]$. In order to exclude a first order process, we performed multiple experiments at selected temperatures using different DMS concentration. By plotting the obtained k_{obs} against concentrations, we obtained a straight line with no significant 0th order term (see supplementary material Figure S3†). In order to calculate the activation parameters, $\ln k$ was fitted against $1/T$, obtaining a straight line with equation $\ln(k/T) = \Delta H^\ddagger/R(1/T) + \Delta S^\ddagger/R + \ln(k_B/h)$. ΔG^\ddagger were calculated at 298.15 K according to the equation $\Delta G^\ddagger = \Delta H^\ddagger - T\Delta S^\ddagger$. All data were fitted with the computer program OriginPro 8 by OriginLab Corporation on a PC running Windows.

X-Ray crystallography

A summary of data collections and structure refinements is reported in Table 4 and Table 5. Single crystal data were collected on a Philips PW 1100 diffractometer (**1a**, **2a**, **1b**), on Bruker Smart 1000 area detector diffractometer (**1c**, **2c**), and on Bruker Smart APEXII area detector diffractometer (**2b**). All data collection were performed with the Mo $K\alpha$ radiation ($\lambda = 0.71073$ Å). For **1a**, **2a** and **1b** the cell constants were obtained from a least-square refinement of the setting angles of 24 randomly distributed and carefully centered reflections, whereas for **1c** and **2c** the cell constants were obtained from a least-square refinement of 10944, and 14330 reflections, respectively. Empirical absorption correction was applied using the program NEWABS923³³ (**1a**, **2a**, **1b**), and with the program SADABS (**1c**, **2c**).³⁴ The crystals of **2b** were identified as non-merohedral twins using RLATT.³⁵ Two unit cells could be determined where the twin law corresponds to $[-1\ 0\ 0, 0\ -1\ 0, 0.35\ 0\ 1]$. Integration of the data of **2b** was performed with SAINT-Plus³⁶ using both orientation matrices. The absorption correction for **2b** was applied using the program TWINABS,³⁷ and each component was scaled separately. The $R(\text{int})$ (point group $2/m$) for the first component refined to 0.0651, and for the second component it refined to 0.0648. Equivalent reflections were merged if they derived from the same twin component. The ratio

of the twin components was refined to 0.87/0.13. The structures of all compounds were solved by direct methods (SIR97³⁸ and SIR2004³⁹), and refined with full-matrix least-squares (SHELX-97),⁴⁰ using the WinGX software package.⁴¹ Non-hydrogen atoms were refined anisotropically for all compounds, and the hydrogen atoms were placed at their calculated positions. Graphical material was prepared with the ORTEP3 for Windows⁴² and Mercury CSD 2.0⁴³ programs. Full tables of bond lengths and angles, atomic positional parameters, anisotropic displacement parameters are given in the supplementary material. Details of the crystal structure investigations (excluding structure factors) are deposited in the Cambridge Crystallographic Data Centre: CCDC 713088–713093.†

Notes and references

- 1 D. Wang and S. J. Lippard, *Nat. Rev. Drug Disc.*, 2005, **4**, 307–320.
- 2 S. A. De Pascali, P. Papadia, A. Ciccarese, C. Pacifico and F. P. Fanizzi, *Eur. J. Inorg. Chem.*, 2005, **4**, 788–796.
- 3 A. Muscella, N. Calabriso, S. A. De Pascali, L. Urso, A. Ciccarese, F. P. Fanizzi, D. Migoni and S. Marsigliante, *Biochem. Pharmacol.*, 2007, **74**(1), 28–40.
- 4 A. Muscella, N. Calabriso, F. P. Fanizzi, S. A. De Pascali, L. Urso, A. Ciccarese, D. Migoni and S. Marsigliante, *Br. J. Pharmacol.*, 2008, **153**, 34–49.
- 5 D. Gibson, J. Lewis and C. Oldham, *J. Chem. Soc. A*, 1967, **1**, 72–77.
- 6 B. N. Figgis, J. Lewis, R. F. Long, R. Mason, R. S. Nyholm, P. J. Pauling and G. B. Robertson, *Nature*, 1962, **195**, 1278–1279.
- 7 F. Basolo, *Coord. Chem. Rev.*, 1996, **154**, 151–161, and references cited therein.
- 8 F. P. Fanizzi, N. Margiotta, M. Lanfranchi, A. Tiripicchio, G. Pacchioni and G. Natile, *Eur. J. Inorg. Chem.*, 2004, **8**, 1705–1713.
- 9 P. D. Braddock, R. Romeo and M. L. Tobe, *Inorg. Chem.*, 1974, **13**(5), 1170–1175.
- 10 L. Cattalini, F. Guidi and M. L. Tobe, *J. Chem. Soc. Dalton Trans.*, 1993, **2**, 233–236.
- 11 P. Nilsson, F. Plamper and O. F. Wendt, *Organometallics*, 2003, **22**(25), 5235–5242.
- 12 O. F. Wendt, K. Oskarsson, J. G. Leipoldt and L. I. Elding, *Inorg. Chem.*, 1997, **36**(20), 4514–4519.
- 13 C. Eaborn, K. Kundu and A. Pidcock, *J. Chem. Soc. Dalton Trans.*, 1981, **4**, 933–938.
- 14 R. Romeo, A. Grassi and L. Monsù Scolaro, *Inorg. Chem.*, 1992, **31**(21), 4383–4390.
- 15 G. Hulley, B. F. G. Johnson and J. Lewis, *J. Chem. Soc. A*, 1970, **10**, 1732–1738.
- 16 M. Bonivento, L. Cattalini, G. Marangoni, G. Michelon, A. P. Schwab and M. L. Tobe, *Inorg. Chem.*, 1980, **19**, 1743–1746.
- 17 M. Bonivento, L. Canovese, L. Cattalini, G. Marangoni, G. Michelon and M. L. Tobe, *Inorg. Chem.*, 1981, **20**, 3728–3730.
- 18 T. Ito, T. Kiriyama and A. Yamamoto, *Bull. Chem. Soc. Jpn.*, 1976, **49**, 3250–3256.
- 19 T. Ito, T. Kiriyama, Y. Nakamura and A. Yamamoto, *Bull. Chem. Soc. Jpn.*, 1976, **49**, 3257–3264.
- 20 S. Baba, T. Ogura and S. Kawaguchi, *Bull. Chem. Soc. Jpn.*, 1974, **47**(3), 665–668.
- 21 A. C. Jesse, D. J. Stufkens and K. Vrieze, *Inorg. Chim. Acta*, 1979, **32**, 87–91.
- 22 J. Ashley-Smith, Z. Douek, B. F. G. Johnson and J. Lewis, *J. Chem. Soc. Dalton*, 1974, **2**, 128–133.
- 23 C. E. Holloway, G. Hulley, B. F. G. Johnson and J. Lewis, *J. Chem. Soc. A*, 1970, **10**, 1653–1658.
- 24 P. S. Pregosin, *Coord. Chem. Rev.*, 1982, **44**, 247–291.
- 25 S. A. Cotton, *Chemistry of Precious Metals*, Blackie Academic and Professional, 1997, London, UK.
- 26 F. P. Fanizzi, N. Margiotta, M. Lanfranchi, A. Tiripicchio, G. Pacchioni and G. Natile, *Eur. J. Inorg. Chem.*, 2004, **8**, 1705–1713.
- 27 F. P. Fanizzi, N. Margiotta, M. Lanfranchi, A. Tiripicchio, G. Pacchioni and G. Natile, *Eur. J. Inorg. Chem.*, 2004, **8**, 1705–1713.
- 28 When the complex and ligand were both soluble, the reactions were performed also in D₂O, giving the same outcome.
- 29 F. P. Fanizzi, F. P. Intini, L. Maresca, G. Natile and G. Uccello-Barretta, *Inorg. Chem.*, 1990, **29**(1), 29–33.
- 30 F. P. Fanizzi, L. Maresca, G. Natile, M. Lanfranchi, A. M. Manotti-Lanfredi and A. Tiripicchio, *Inorg. Chem.*, 1988, **27**(14), 2422–31.
- 31 R. K. Harris, E. D. Becker, S. M. Cabral De Menezes, R. Goodfellow and P. Granger, *Pure Appl. Chem.*, 2001, **73**, 1795–1818.
- 32 R. Romeo, D. Minniti, S. Lanza and M. L. Tobe, *Inorg. Chim. Acta*, 1977, **22**, 87–91.
- 33 (a) N. Walker and D. Stuart, *Acta Crystallogr. Sect. A*, 1983, **39**, 158; (b) F. Ugozzoli, *Comput. Chem.*, 1987, **11**, 109.
- 34 *Area-Detector Absorption Correction*, Siemens Industrial Automation, Inc., Madison, WI, (1996).
- 35 *RLATT*, Bruker, AXS Inc., Madison, Wisconsin, USA.
- 36 *SAINT-Plus (Version 7.51A)*, Bruker AXS Inc., Madison, Wisconsin, USA.
- 37 G. M. Sheldrick, (2007). *TWINABS (Version 2007/5)*, University of Göttingen, Germany.
- 38 A. Altomare, M. C. Burla, M. Camalli, G. L. Cascarano, C. Giacovazzo, A. Guagliardi, A. G. G. Moliterni, G. Polidori and R. J. Spagna, *Appl. Crystallogr.*, 1999, **32**, 115.
- 39 M. C. Burla, R. Caliandro, M. Camalli, B. Carrozzini, G. L. Cascarano, L. De Caro, C. Giacovazzo, G. Polidori and R. Spagna, *J. Appl. Crystallogr.*, 2005, **38**, 381–388.
- 40 G. M. Sheldrick, *SHELX97. Programs for Crystal Structure Analysis (1997) (release 97-2)*, University of Göttingen, Germany.
- 41 L. J. Farrugia, *Appl. Crystallogr.*, 1999, **32**, 837.
- 42 L. J. Farrugia, *J. Appl. Crystallogr.*, 1997, **30**, 565.
- 43 C. F. Macrae, P. R. Edgington, P. McCabe, E. Pidcock, G. P. Shields, R. Taylor, M. Towler and J. van de Streek, *J. Appl. Crystallogr.*, 2006, **39**, 453–457.